JOURNAL OF APPLIED PHYSICS **104**, 063114 (2008)

Influence of applied electric fields on the absorption coefficient and subband energy distances of intersubband transitions in AlN/GaN coupled double quantum wells

L. B. Cen, B. Shen,[a] Z. X. Qin, and G. Y. Zhang
State Key Laboratory of Artificial Microstructure and Mesoscopic Physics, School of Physics, Peking University, Beijing 100871, People's Republic of China

(Received 3 June 2008; accepted 18 July 2008; published online 26 September 2008)

The influence of applied electric fields on the absorption coefficient and subband energy distances of intersubband transitions (ISBTs) in AlN/GaN coupled double quantum wells (CDQWs) has been investigated by solving the Schrödinger and Poisson equations self-consistently. It is found that the absorption coefficient of the ISBT between the ground state and the second excited state $(1_{\text{odd}}-2_{\text{odd}})$ can be equal to zero when the electric fields are applied in AlN/GaN CDQWs, which is related to the applied electric field induced symmetry recovery of these states. Meanwhile, the energy distances between $1_{\text{odd}}-2_{\text{odd}}$ and $1_{\text{even}}-2_{\text{odd}}$ subbands have different relationships from each other with the increase of applied electric fields due to the different polarization-induced potential drops between the left and right wells. The results indicate that an electrical-optical modulator operated within the optocommunication wavelength range can be realized in spite of the strong polarization-induced electric fields in AlN/GaN CDQWs. © *2008 American Institute of Physics*.
[DOI: 10.1063/1.2980320]

I. INTRODUCTION

The intersubband transitions (ISBTs) in semiconductor quantum wells (QWs) are of high significance for both fundamental physics research and the application for optoelectronics due to the ultrafast carrier relaxation dynamics. Linear and nonlinear intersubband optical absorptions and the confined structures of Radovanovic *et al.*[1–3] are full of interest. Owing to the large LO-phonon energy in GaN-based materials, the ISBTs in $Al_xGa_{1-x}N/GaN$ QWs have an ultrashort carrier relaxation time than the $Al_xGa_{1-x}As/GaAs$ ones.[4–8] Meanwhile, the wavelengths of the ISBTs in $Al_xGa_{1-x}N/GaN$ QWs can be shorter than the $Al_xGa_{1-x}As/GaAs$ ones due to the large conduction band offsets at $Al_xGa_{1-x}N/GaN$ heterointerfaces.[9]

Although the above-mentioned advantages of $Al_xGa_{1-x}N/GaN$ QWs are much useful to realize an electrical-optical modulator operated within the optocommunication wavelength range, the polarization-induced electric fields lead to a potential drop between the left and right wells, and thus, result in Stark shift between the subbands in the two wells in spite of the same thickness and depth chosen for the two wells in $Al_xGa_{1-x}N/GaN$ coupled double quantum wells (CDQWs).[10] Therefore, the dipole matrix element of the ISBT between the ground state and the second excited state $(1_{\text{odd}}-2_{\text{odd}})$ is not equal to zero. In this study, the influence of applied electric fields on the absorption coefficient and subband energy distances of the ISBTs in AlN/GaN CDQWs has been investigated by solving the Schrödinger and Poisson equations self-consistently. The results indicate that an electrical-optical modulator operated within the optocommunication wavelength range can be realized in spite of the strong polarization-induced electric fields in AlN/GaN CDQWs.

II. THEORETICAL CALCULATION

The absorption coefficient of the ISBTs in the conduction band of AlN/GaN CDQWs can be expressed as a function of ω by the following formula:[11,12]

$$\alpha(\omega) = \frac{\omega}{\mathrm{L}}\sqrt{\frac{\mu_0}{\varepsilon_0\varepsilon_r}}\sum_{m>n}\frac{|\mathrm{M}_{mn}|^2[N_n - N_m](\hbar/\tau)}{[E_m - E_n - \hbar\omega]^2 + (\hbar/\tau)^2}, \tag{1}$$

where μ_0 is the permeability in vacuum, ε_0 is the dielectric constant in vacuum, ε_r is the relative dielectric constant, L is the total QW width, $\hbar$ is the reduced Planck constant, τ is the dephasing time, and M_{mn} is the dipole matrix. τ is assumed to be 0.14 ps in the calculation.[12] M_{mn} is given by

$$M_{mn} = \int_{-L/2}^{L/2}\psi_m^*(z)ez\psi_n(z)dz, \tag{2}$$

where e is the electronic charge, N_i is the total electrons resided in the ith subband level, and E_i and ψ_i $(i=m,n)$ are the energy level and the wave function of the ith subband, respectively. They are obtained by solving the Schrödinger and Poisson equations self-consistently

$$-\frac{\hbar^2}{2}\frac{d}{dz}\left[\frac{1}{m^*(z)}\frac{d}{dz}\psi_i(\mathrm{z})\right] + \left[\mathrm{V}(z) + \frac{\Delta E_c}{e} + \mathrm{V}_{\mathrm{xc}}(z) - e\phi_H(z)\right]\psi_i(z) = E_i\psi_i(z), \tag{3}$$

[a]Electronic mail: bshen@pku.edu.cn.

 © 2008 American Institute of Physics

$$\frac{d}{dz}\left[\varepsilon_0\varepsilon_r\frac{d}{dz}\phi_H(z)\right] = -e[N_D^+(z) - n_{2D}(z) - n_{3D}(z)], \quad (4)$$

$$V_{xc}(z) = -0.985\frac{e^2}{4\pi\varepsilon_0\varepsilon_r}n^{1/3}(z) \times\left\{1 + \frac{0.034}{\alpha_H^* n^{1/3}(z)}\ln[1 + 18.376 a_H^* n^{1/3}(z)]\right\}, \quad (5)$$

where z is the space coordinate along the growth direction, $m^*(z)$ is the position-dependent effective mass, $V(z)$ is the applied voltage, ΔE_c is the conduction band offset, $\phi_H(z)$ is the Hartree potential due to the electrostatic interaction, $V_{xc}(z)$ is the exchange correlation potential,[13] $a_H^* = 4\pi\varepsilon_0\varepsilon_r\hbar^2/m^*(z)e^2$,[14] $N_D^+(z)$ is the ionized donor density, $n_{2D}(z)$ is the two-dimensional electron density in all subbands, $n_{3D}(z)$ is the three-dimensional (3D) electron density, and $n(z)$ is the sum of $n_{2D}(z)$ and $n_{3D}(z)$. Under the equilibrium condition, $n_{2D}(z)$, $n_{3D}(z)$, and N_i are given by the formulas as follows:[14]

$$n_{2D}(z) = \sum_i n_{2D_i}(z) = \sum_i \frac{m^* KT}{\pi\hbar^2}|\psi_i(z)|^2 \ln\left[1 + \exp\left(\frac{E_f - E_i}{KT}\right)\right], \quad (6)$$

$$n_{3D}(z) = N_C(z) F_{1/2}\left(\frac{E_f - E_i}{KT}\right), \quad (7)$$

$$N_i = \int n_{2D_i}(z)dz, \quad (8)$$

where K is the Boltzmann constant, T is the absolute temperature, m^* is the effective mass of electron (for simplicity, a same effective mass is used in the well), E_F is the Fermi level, $N_C(z)$ is the 3D density of states, and $F_{1/2}$ is the Fermi–Dirac integral. In the calculation, the initial potential profile is assumed to be a rectangular potential profile. In order to ensure constringency of solving the Schrödinger and Poisson equations self-consistently, the potential profile of the next iteration is recalculated from a linear combination of new and old values of the potential profiles. The detailed self-consistent procedure can be found in the literature.[15]

In the calculation, the band gap is chosen as 3.4 eV for GaN and 6.2 eV for AlN.[16] The conduction band offset is assumed to be 70% of the total band offset.[16] The minimum of the conduction band profile of AlN/GaN CDQWs is defined as the zero reference energy. Under the assumption of the periodic potential model, the charge neutrality condition is adopted, which means that the sum of the charges in a periodic AlN/GaN CDQWs is zero. The relationships between the total polarization field discontinuity (ΔP) and the polarization-induced electric fields in the barriers and the wells are expressed as[14]

$$F_1 = \frac{(\varepsilon_3\varepsilon_4 l_2 + \varepsilon_2\varepsilon_4 l_3 + \varepsilon_2\varepsilon_3 l_4)\Delta P_1 + (\varepsilon_2\varepsilon_4 l_3 + \varepsilon_2\varepsilon_3 l_4)\Delta P_2 + \varepsilon_2\varepsilon_3 l_4 \Delta P_3}{\varepsilon_0(\varepsilon_2\varepsilon_3\varepsilon_4 l_1 + \varepsilon_1\varepsilon_3\varepsilon_4 l_2 + \varepsilon_1\varepsilon_2\varepsilon_4 l_3 + \varepsilon_1\varepsilon_2\varepsilon_3 l_4)}, \quad (9)$$

$$F_2 = \frac{\varepsilon_3\varepsilon_4 l_1 \Delta P_1 - (\varepsilon_1\varepsilon_4 l_3 + \varepsilon_1\varepsilon_3 l_4)\Delta P_2 - \varepsilon_1\varepsilon_3 l_4 \Delta P_3}{\varepsilon_0(\varepsilon_2\varepsilon_3\varepsilon_4 l_1 + \varepsilon_1\varepsilon_3\varepsilon_4 l_2 + \varepsilon_1\varepsilon_2\varepsilon_4 l_3 + \varepsilon_1\varepsilon_2\varepsilon_3 l_4)}, \quad (10)$$

$$F_3 = \frac{\varepsilon_2\varepsilon_3 l_1 \Delta P_1 + (\varepsilon_2\varepsilon_4 l_1 + \varepsilon_1\varepsilon_4 l_2)\Delta P_2 - \varepsilon_1\varepsilon_2 l_4 \Delta P_3}{\varepsilon_0(\varepsilon_2\varepsilon_3\varepsilon_4 l_1 + \varepsilon_1\varepsilon_3\varepsilon_4 l_2 + \varepsilon_1\varepsilon_2\varepsilon_4 l_3 + \varepsilon_1\varepsilon_2\varepsilon_3 l_4)}, \quad (11)$$

$$F_4 = \frac{\varepsilon_2\varepsilon_3 l_1 \Delta P_1 + (\varepsilon_2\varepsilon_3 l_1 + \varepsilon_1\varepsilon_3 l_2)\Delta P_2 + (\varepsilon_2\varepsilon_3 l_1 + \varepsilon_1\varepsilon_3 l_2 + \varepsilon_1\varepsilon_2 l_3)\Delta P_3}{\varepsilon_0(\varepsilon_2\varepsilon_3\varepsilon_4 l_1 + \varepsilon_1\varepsilon_3\varepsilon_4 l_2 + \varepsilon_1\varepsilon_2\varepsilon_4 l_3 + \varepsilon_1\varepsilon_2\varepsilon_3 l_4)}, \quad (12)$$

where F_1 is the polarization-induced electric field in the left barrier, F_2 is the polarization-induced electric field in the left well, F_3 is the polarization-induced electric field in the central coupled barrier, F_4 is the polarization-induced electric field in the right well, l_1 is the thickness of the left barrier, l_2 is the thickness of the left well, l_3 is the thickness of the central coupled barrier, l_4 is the thickness of the right well, ε_0 is the dielectric constant in vacuum, ε_1 is the relative dielectric constant of the left barrier, ε_2 is the relative dielectric constant of the left well, ε_3 is the relative dielectric constant of the central coupled barrier, ε_4 is the relative dielectric constant of the right well, ΔP_1 is the polarization field discontinuity at the heterointerface between the left barrier and the left well, ΔP_2 is the polarization field discontinuity at the heterointerface between the left well and the central coupled barrier, and ΔP_3 is the polarization field discontinuity at the heterointerface between the central coupled barrier and the right well.

III. RESULTS AND DISCUSSION

The structure of AlN/GaN CDQWs used in the calculation is 10 nm AlN/1.5 nm GaN/1 nm AlN/1.5 nm GaN. The total polarization field discontinuities (ΔP) are assumed as

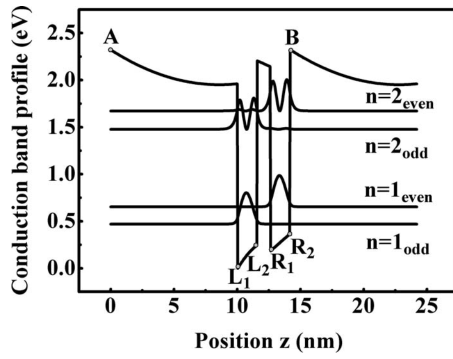

FIG. 1. Schematic conduction band profile of AlN/GaN CDQWs and the moduli square of the wave functions under zero-applied electric fields.

follows:[14] $\Delta P_1 = 2$ MV/cm, $\Delta P_2 = -1.74$ MV/cm, and $\Delta P_3 = -\Delta P_2$. The doping concentration in the left barrier is assumed to be 5×10^{18} cm^{-3}. Dot L_1 is the reference energy, which is defined as zero. Electric fields are applied between dots A and B. Figure 1 shows the schematic conduction band profile of AlN/GaN CDQWs and the moduli square of the wave functions under zero-applied electric fields. As shown in Fig. 1, the polarization field induced potential drops lead to the asymmetry of the conduction band profile, and thus, result in Stark shifts between the resonance subbands in AlN/GaN CDQWs. This leads to the decrease of the tunneling probability of the electrons in the left and right wells between each other. The wave functions of the odd order subbands (1_{odd} and 2_{odd}) are mainly located in the left well, and those of the even order subbands (1_{even} and 2_{even}) are mainly located in the right one. As compared to symmetric CDQWs, the 1_{odd} and 2_{odd} wave functions are not even symmetric and the absorption coefficient of $1_{odd}-2_{odd}$ ISBT is not equal to zero in AlN/GaN CDQWs under zero-applied electric fields.

Figure 2 shows the absorption coefficient of $1_{odd}-2_{odd}$ ISBT as a function of applied electric fields in AlN/GaN CDQWs. It is found that the absorption coefficient of $1_{odd}-2_{odd}$ ISBT is equal to zero when the applied electric field is equal to 1.05 MV/cm. The zero-absorption coefficient of $1_{odd}-2_{odd}$ ISBT is not attributed to a reduced overlap of the final and initial states of the transition (quantum confined stark effect)[17] because it remains equal to zero even if the overlap of the final and initial states of $1_{odd}-2_{odd}$ ISBT is reduced to zero by the applied electric field. This phenom-

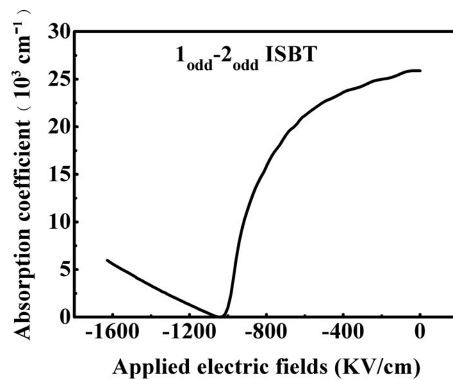

FIG. 2. The absorption coefficient of $1_{odd}-2_{odd}$ ISBT as a function of applied electric fields in AlN/GaN CDQWs.

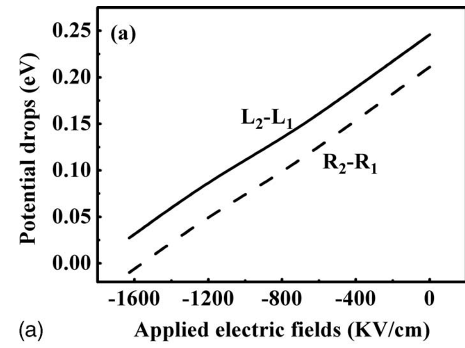

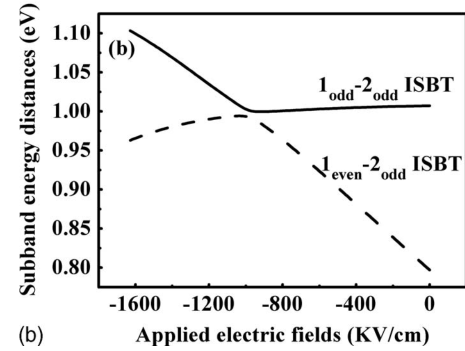

FIG. 3. (a) Potential drops in the left and right wells as a function of applied electric fields and (b) the energy distances between $1_{odd}-2_{odd}$ and $1_{even}-2_{odd}$ subbands as a function of applied electric fields in AlN/GaN CDQWs.

enon can be explained as follows: AlN/GaN CDQWs can be considered as two isolated wells, defined here as wells a and b, coupled by the central barrier. The wave functions of this system can be expanded in terms of the wave functions of the first two bound states $|\varphi_j\rangle$ $(j=1,2)$ of the two isolated wells. The dipole matrix element of $1_{odd}-2_{odd}$ ISBT in AlN/GaN CDQWs can be written as the sum of the contribution from the two wells a and b

$$\langle 1_{odd}|z|2_{odd}\rangle = \langle 1_{odd}|\varphi_1^a\rangle\langle 2_{odd}|\varphi_2^a\rangle z_{12}^a + \langle 1_{odd}|\varphi_1^b\rangle \times\langle 2_{odd}|\varphi_2^b\rangle z_{12}^b, \tag{13}$$

where z_{12}^a and z_{12}^b are the dipole matrix elements of the isolated wells. As $|1_{odd}\rangle$ is the ground state of the coupled system, $\langle 1_{odd}|\varphi_1^a\rangle$ and $\langle 1_{odd}|\varphi_1^b\rangle$ have the same sign. However, since the second excited state $|2_{odd}\rangle$ crosses zero twice and is constructed from the asymmetric wave functions $|\varphi_2^a\rangle$ and $|\varphi_2^b\rangle$, $\langle 2_{odd}|\varphi_2^a\rangle$ and $\langle 2_{odd}|\varphi_2^b\rangle$ have opposite signs. Therefore, corresponding to $1_{odd}-2_{odd}$ ISBT in AlN/GaN CDQWs, the two terms of Eq. (13) have opposite signs. When a large electric field is applied, the 1_{odd} and 2_{odd} wave functions are mainly localized in the same well. As a result, only one term of Eq. (13) plays the dominant role and large value of $\langle 1_{odd}|z|2_{odd}\rangle$ is obtained. On the contrary, when some intermediate value of electric field is applied, two terms of Eq. (13) play the role, which have opposite contributions to the transition. Then, a null is expected for the dipole matrix element $\langle 1_{odd}|z|2_{odd}\rangle$.

Figure 3(a) shows the different potential drops in the left and right wells as a function of applied electric fields, respectively. Figure 3(b) shows the energy distances of $1_{odd}-2_{odd}$ and $1_{even}-2_{odd}$ subbands as a function of applied electric

fields, respectively. As shown in Fig. 3(a), the potential drop in the right well (curve R_2-R_1) is always smaller than that in the left one (curve L_2-L_1) when applied electric fields increase. It results in the subband energy levels in the left well having smaller shifts than those in the right one with the increase of applied electric fields in AlN/GaN CDQWs. As shown in Fig. 3(b), the energy distance between $1_{odd}-2_{odd}$ subbands decreases while that between $1_{even}-2_{odd}$ ones increases with the increase of applied electric fields. Such phenomenon can be attributed to the different polarization-induced potential drops in the left and right wells. When the applied electric field is zero, the 1_{odd} and 2_{odd} wave functions are mainly located in the left well while the 1_{even} and 2_{even} wave functions are mainly located in the right one. The energy distance between $1_{odd}-2_{odd}$ subbands decreases while that between $1_{even}-2_{odd}$ ones increases with the increase in applied electric fields. However, when the applied electric field is large enough to change the 1_{odd} and 1_{even} wave functions between the left and right wells, the energy level shifts of 1_{odd} and 2_{even} subbands are larger than those of 1_{even} and 2_{odd} ones with the increase of applied electric fields. The subband energy distance between $1_{even}-2_{odd}$ subbands decreases while that between $1_{odd}-2_{odd}$ ones increases with the increase of applied electric fields.

IV. CONCLUSIONS

In conclusion, the influence of applied electric fields on the absorption coefficient and subband energy distances of the ISBTs in AlN/GaN CDQWs has been investigated by solving the Schrödinger and Poisson equations self-consistently. The absorption coefficient of $1_{odd}-2_{odd}$ ISBT can be equal to zero when the electric fields are applied in AlN/GaN CDQWs, which is related to the applied electric field induced symmetry recovery of these states. Meanwhile, the energy distances between $1_{odd}-2_{odd}$ and $1_{even}-2_{odd}$ subbands have different relationships from each other with the increase of applied electric fields due to the different polarization-induced potential drops between the left and right wells. The results indicate that an electrical-optical modulator operated within the optocommunication wavelength range can be realized in spite of the strong polarization-induced electric fields in AlN/GaN CDQWs.

ACKNOWLEDGMENTS

This work was supported by the National Natural Science Foundation of China (Grant Nos. 60628402, 10774001, and 60736033), the National Basic Research Program of China (Grant Nos. 2006CB604908 and 2006CB921607), the Cultivation Fund of the Key Scientific and Technical Innovation Project, Ministry of Education of China (Grant No. 705002), the Research Fund for the Doctoral Program of Higher Education in China (Grant No. 20060001018), and the Beijing Natural Science Foundation (Grant No. 4062017).

[1] J. Radovanovic, V. Milanovic, D. Indjin, and Z. Ikonic, J. Appl. Phys. **92**, 7672 (2002).
[2] J. Radovanovic, V. Milanovic, Z. Ikonic, D. Indjin, V. Jovanovic, and P. Harrison, IEEE J. Quantum Electron. **39**, 1297 (2003).
[3] J. Radovanovic, V. Milanovic, Z. Ikonic, and D. Indjin, Phys. Rev. B **69**, 115311 (2004).
[4] A. Othonos, J. Appl. Phys. **83**, 1789 (1998).
[5] S. Rudin and T. L. Reinecke, Phys. Rev. B **41**, 7713 (1990).
[6] N. Iizuka, K. Kaneko, N. Suzuki, T. Asano, S. Noda, and O. Wada, Appl. Phys. Lett. **77**, 648 (2000).
[7] N. Suzuki and N. Iizuka, Jpn. J. Appl. Phys., Part 2 **36**, L1006 (1997).
[8] C. Gmachl, S. V. Frolov, H. M. Ng, S. N. G. Chu, and A. Y. Cho, Electron. Lett. **37**, 378 (2001).
[9] C. Gmachl, H. M. Ng, and A. Y. Cho, Appl. Phys. Lett. **77**, 334 (2000).
[10] S. Y. Lei, B. Shen, L. Cao, F. J. Xu, Z. J. Yang, K. Xu, and G. Y. Zhang, J. Appl. Phys. **99**, 074501 (2006).
[11] A. Sa'ar and R. Kapon, IEEE J. Quantum Electron. **33**, 1517 (1997).
[12] D. Ahn and S. L. Chuang, IEEE J. Quantum Electron. **23**, 2196 (1987).
[13] L. Brey, J. Dempsey, N. F. Johnson, and B. I. Halperin, Phys. Rev. B **42**, 1240 (1990).
[14] S. Y. Lei, B. Shen, L. Cao, Z. J. Yang, and G. Y. Zhang, J. Appl. Phys. **101**, 123108 (2007).
[15] A. Abou-Elnour and K. Schuenemann, J. Appl. Phys. **74**, 3273 (1993).
[16] O. Ambacher, J. Smart, J. R. Shealy, N. G. Weimann, K. Chu, M. Murphy, W. J. Schaff, L. F. Eastman, R. Dimitrov, L. Wittmer, M. Stutzmann, W. Rieger, and J. Hilsenbeck, J. Appl. Phys. **85**, 3222 (1999).
[17] T. Takeuchi, C. Wetzel, S. Yamaguchi, H. Sakai, H. Amano, and I. Akasaki, Appl. Phys. Lett. **73**, 1691 (1998).

Journal of Applied Physics is copyrighted by the American Institute of Physics (AIP). Redistribution of journal material is subject to the AIP online journal license and/or AIP copyright. For more information, see http://ojps.aip.org/japo/japcr/jsp